used, as some of D_{ijr} can be obtained from the others by (9) and (10).

Once all the D_{ijk} are calculated, the next task is to calculate h_j, k_j, l_j from them. This can be best accomplished by using some of 35 equations of four terms each, exemplified by

$$x_1D_{234}-x_2D_{134}+x_3D_{124}-x_4D_{123}=0 \qquad (13)$$

where three independent solutions in x stand in turn for h, then k, then l.

Because there is an ambiguity in the choice of axes in a triclinic case, three hkl points can be freely chosen subject to one condition (13) and four others can be calculated from these. In this way, any one set of 21 Miller indices can be readily calculated. The one set of Miller indices will be one member of the infinite set obtainable by unimodular transformations. Again, not all the 35 equations (13) need be used, but only enough to determine all the Miller indices of the required set.

Conclusions

The above mathematics may appear too complex to an ordinary powder-diffractionist to be of any practical use, but the greatest practical computational problem is the solution of equation (5) in integers within observational tolerances. Once this equation is solved, all the rest of the equations deal in integers, are therefore exact, and are easier to solve than equation (5).

The treatment greatly simplifies when crystal systems of higher symmetry are considered. The hexagonal and tetragonal systems can be solved at once by the aid of a simple nomograph, and the solution of the orthorhombic system requires only a moderate computational effort. However, the monoclinic and the triclinic case will require the use of a computer.

This paper was written in connection with information-retrieval studies supported by the Joint Committee on Powder Diffraction Standards through the American Society for Testing and Materials (Pennsylvania State University Grant 2212). Moral encouragement as well as financial support is gratefully acknowledged.

References

AZAROFF, L. V. & BUERGER, M. J. (1958). *The Powder Method in X-ray Crystallography*. New York: McGraw-Hill.
BUERGER, M. J. (1957). *Z. Kristallogr.* **109**, 42.
HESSE, R. (1948). *Acta Cryst.* **1**, 200.
ITO, T. (1950). *X-ray Studies on Polymorphism*. Tokyo: Maruzen.
LIPSON, H. (1949). *Acta Cryst.* **2**, 43.
RUNGE, C. (1917). *Phys. Z.* **18**, 509.
STOSICK, A. J. (1949). *Acta Cryst.* **2**, 271.
TURNBULL, H. W. (1960). *The Theory of Determinants, Matrices and Invariants*. New York: Dover.
VAND, V. (1948). *Acta Cryst.* **1**, 109, 290.
WOLFF, P. M. DE (1957). *Acta Cryst.* **10**, 590.
WOLFF, P. M. DE (1958). *Acta Cryst.* **11**, 664.
WOLFF, P. M. DE (1967). Personal communication.

Acta Cryst. (1968). A**24**, 546

A Study of Optimal Phase Boundaries: The Case of Exsolved Alkali Feldspars

BY W. BOLLMANN
Battelle Institute Advanced Studies Center, Geneva, Switzerland

AND H.-U. NISSEN
Institut für Kristallographie und Petrographie, ETH, Zürich, Switzerland

(*Received* 28 *December* 1967 *and in revised form* 22 *February* 1968)

A general theory of grain and phase boundaries (the *O*-lattice theory) is further developed and tested on alkali feldspars with exsolution lamellae, since measurements exist for the structures of the two-phase system (perthitic feldspars) as well as for the orientation of the phase boundary. It is shown that in this case the adaptation of two monoclinic structures is energetically preferable to the adaptation of a monoclinic and a triclinic one. The phase boundary energy is markedly lower in the former case. Thus, a pseudo-monoclinic structure is produced out of the triclinic by periodic submicroscopic twinning. The calculated orientation of the phase boundary is in close agreement with the measurements.

Introduction

Since most materials are polycrystalline, the importance of the study of crystal interfaces does not need to be emphasized. One usually distinguishes between subgrain boundaries consisting of distinct dislocation networks and high-angle boundaries where a dislocation density would be so high that the dislocation cores would merge so that at first sight a boundary might appear as a highly disturbed interface. A distinction is also made between boundaries of the same material (grain boundaries) and of different materials (phase boundaries).

The theory of subgrain boundaries was developed by Read and Shockley (Read, 1963) with the accent on energy and by Frank (1950) more from the point of view of geometry. A review on subgrain boundaries is given by Amelinckx & Dekeyser (1959). Bollmann (1962, 1964) gave a dualistic formulation of the geometry of subgrain boundaries.

The study of the geometry of high-angle boundaries was initiated by Frank (1958) and further developed among others by Brandon (1966) and Ranganathan (1966) based on the concept of the coincidence site lattice. Bollmann (1967) gave a general formalism (the *O*-lattice theory) which can be applied to all kinds of grain and phase boundaries and includes the dislocation networks as well as the coincidence site lattice.

The present paper is considered on one hand as a further development of the *O*-lattice theory by introducing a criterion for an 'optimal' boundary and on the other hand as a numerical test on a monoclinic-triclinic system for which relevant data for the crystal structure as well as the boundary orientation are available. A short introduction to the general theory will be given. However, a full understanding will not be possible without familiarity with the above mentioned basic paper.

The mineralogical problem

The orientation relations in exsolution lamellae of perthite and moonstone have been selected as an application of the theory of phase boundaries to minerals. Perthites and moonstones (cryptoperthites) are a microscopic or submicroscopic association of units of albite, $NaAlSi_3O_8$ and K-feldspar, $KAlSi_3O_8$ (*cf.* Alling, 1932; Laves & Soldatos, 1963). The Na-feldspar phase, which may amount to over 50%, is exsolved in moonstone as parallel lamellae with a periodicity of about 1000 Å producing Bragg diffraction phenomena ('Schiller' or opalescence) in the wavelength range of visible light (Fleet & Ribbe, 1963; Nissen & Bollmann, 1966) (Fig. 1).

The lattice constants of feldspar phases in moonstones must be regarded as slightly abnormal owing to adaptations near the exsolution boundaries (Laves, 1952). The measurement of lattice constants in moonstones is also made difficult by the considerable changes in Na content of the K-feldspar and Ca content of the Na-feldspar phases in different materials as well as in the same specimen. In order to calculate optimal phase boundaries, the lattice constants of the two phases in a moonstone were therefore 'simulated' by using lattice constants of single phases.

To date three kinds of moonstone have been described:

I. Monoclinic or very nearly monoclinic K-feldspar with a low amount of Na is exsolved against nearly equal amounts of low albite submicroscopically twinned after the albite law (twin axis **b***) (Laves, 1952; Fleet & Ribbe, 1963; Nissen & Bollmann, 1966). This type occurs in slowly cooled plutonites (charnockitic rocks, larvikites). These materials may also contain small areas either with twinning after the pericline law or with both albite and pericline twinning (MacKenzie & Smith, 1954).

II. Sanidine with varying Na content has exsolved high albite (Laves, 1952; MacKenzie & Smith, 1955) which is submicroscopically twinned after the pericline law (twin axis **b**). In this type, we have succeeded in finding the twinning domains in electron transmission micrographs.

III. Adularia with submicroscopic 'cryptomicrocline' texture (*cf.* McConnel, 1965) has exsolved albite which is submicroscopically twinned after a combination of the albite and pericline laws (Nissen, 1967. See also Smith & MacKenzie, 1954, 1955; MacKenzie & Smith, 1955; Smith 1961).

The following calculations have been made only for type I. When without the submicroscopic twinning and with exsolved areas which are of at least microscopic dimensions it corresponds to type I of ordinary perthites (Laves & Soldatos, 1963), which form a large portion of granitic and gneiss rocks. The lattice constants assumed for this moonstone must be considered as a model and are, in the natural state, subject to small changes due to variations in Na content, distortion of unit cells near phase boundaries, errors of measurement, *etc.* The lattice constants of 'orthoclase' from Mogok, Burma (Cole, Sørum & Kennard, 1949) with 8 mol% albite component were taken as the K-feldspar phase and those for low albite from Kodarma, Finland (Cole, Sørum & Taylor, 1951) as the Na-feldspar phase. [Similar lattice constants were also given *e.g.* by Orville (1967)].

The full description of the orientation relations along a phase or grain boundary comprises two kinds of data: (1) The relative orientation of the two lattices and (2) the orientation of the phase boundary with respect to the two lattices. Among others, Des Cloizeaux (1862, 1876), Brögger (1890) and Bøggild (1924) measured the angles between the 'lamellae' acting as a diffraction grating and the cleavage. Once the relation between these hypothetical lamellae and cryptoperthitic unmixing was suggested (Brögger, 1890; Kôzu & Endô, 1921; Hadding, 1921†) the index of the mean phase boundary was determined optically for moonstones, taken from 12 localities, to vary approximately between ($\bar{8}01$) and ($\bar{6}01$) (Bøggild, 1924), *i.e.* to be generally non-rational. Nearly the same boundary faces were found by Bøggild in some perthites. A similar phase boundary of exsolved Na-feldspar in perthites and moonstone was described by Schröder (1965) and Michaelis de Sáenz (1965), and Mäkinen (1917) reported ($\bar{6}01$)

---

† The latter papers escaped the attention of Bøggild.

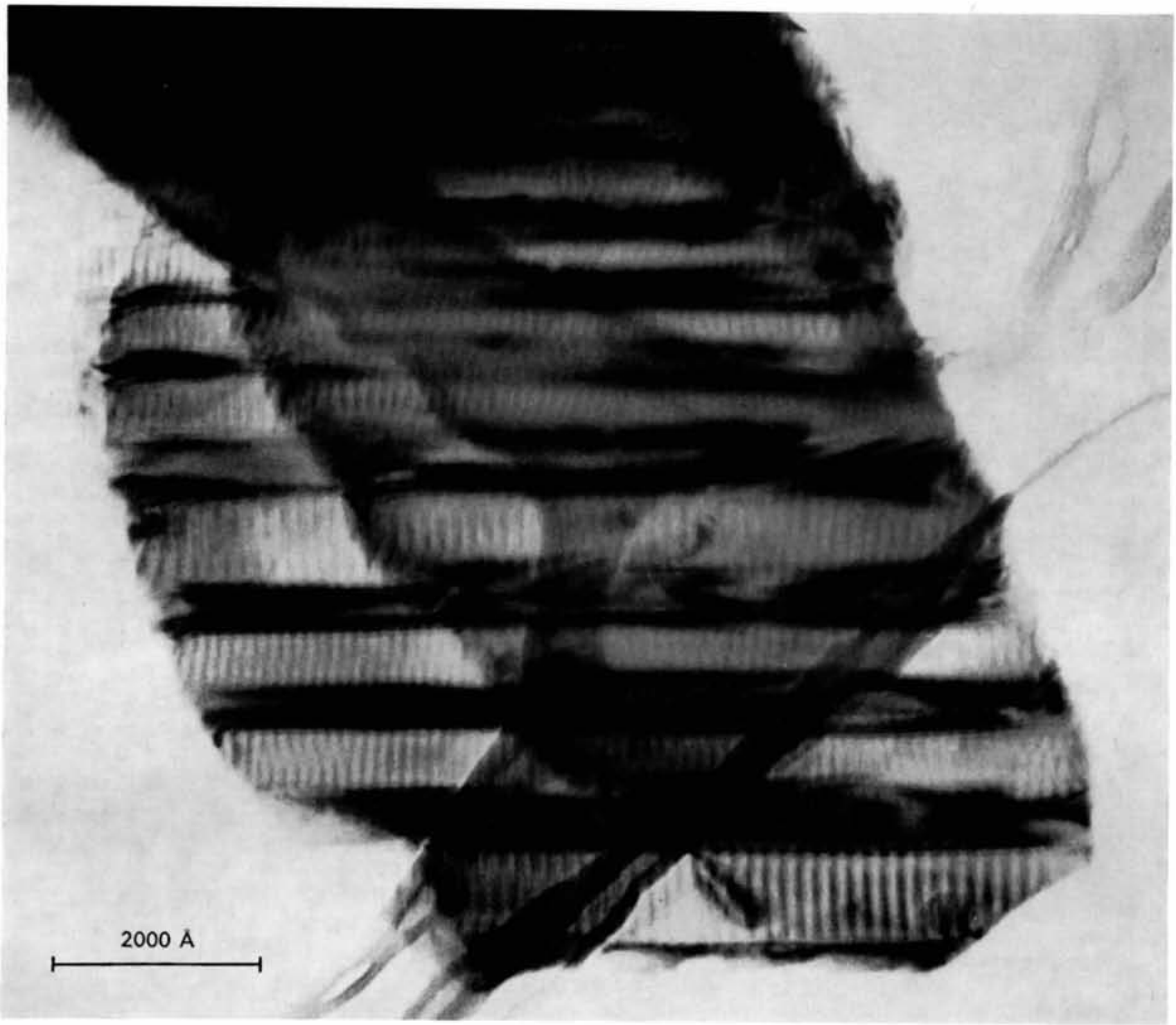

Fig. 1. Cryptoperthite in larvikite (specimen 'Spencer R'). Lamellae of Na-feldspar twinned after the albite law in monoclinic (untwinned) K-feldspar. (Note the relation between the width of the Na-feldspar lamellae and the width of the twin units.)

to ($\bar{8}01$) planes as parting planes of 'murchisonite', a variety of perthite with a non-rational cleavage plane. The relative orientation of the two feldpar lattices was determinded for the first time also by Bøggild (1924). He measured a deviation of 55′ for the *a* axes and calculated a deviation of 19′ for the *c* axes. Laves & Soldatos (1963), using the precession method, corroborated these data.

When comparing the angles between the (001) cleavages of albite and of K-feldspar and the phase boundary in perthites (found to be parallel to the Schiller 'reflexion' plane in moonstone) Bøggild found: '... a very near coincidence, and the values will show, furthermore, that if we go to other faces in the same zone the differences between the two series [*i.e.* of adjacent indices in the two phases] will be larger in both directions ...'. Laves (1952, p. 562–567), using the precession method, measured 60′ difference between the *a* axes and 35′ between the *c* axes of albite and K-feldspar in type I moonstones. He found the same relation between the orientation of the two lattices and the phase boundary in type I moonstone as Bøggild had described for perthites.

Chao & Taylor (1940) found submicroscopic twinning of the Na-feldspar phase as the correct interpretation of additional reflexions which were also treated later by Raman, Jayaraman & Srinivasan (1950), Jayaraman (1959) and Ito & Sadanaga (1951) but partly explained in other ways. Laves (1952) showed that in type I moonstone these additional reflexions are elongated in [b^*] and are produced by albite twinning; in type II moonstone they are elongated in directions between about [106] and [108] and correspond to pericline twinning. He identified the exsolved phase in type II moonstone as high albite. He also described a type I moonstone showing a twinning superstructure with a sixfold *b*-axis repeat, while Saalfeld (1952) found an eightfold repeat and Fleet & Ribbe (1963) a fourfold repeat. Laves wrote that: '... as a result of variability of strain relations ...' several values were found as an average. This can be directly seen from the variability in the thickness of twin units in Fig. 1.

The *O*-lattice

We give here a brief description of the essential points of the *O*-lattice theory. In order to determine a boundary between two crystals, the structure and relative orientation of the two crystals as well as the orientation of the boundary have to be taken into account. We refer here to translation lattices and in more complicated structures only to the geometry of the unit cell. In order to determine the boundary we interpret the two crystals as *interpenetrating lattices*. Then, within the interpenetrating lattices, a boundary will be placed through points where both lattices match best. Once the boundary is chosen, only one lattice on each side is considered as real, so that now two different real crystals are separated by the boundary. The points where the two interpenetrating lattices fit best constitute the *O-lattice.*

When the two lattices (1 and 2) are given, we relate them by a *linear non-degenerate transformation* which in general is *homogeneous*:

$$\mathbf{x}^{(2L)} = \mathbf{A}\mathbf{x}^{(1L)}, \ |\mathbf{A}| \neq 0 \ . \tag{1}$$

We choose lattice 1 as our basic coordinate system so that all values of $\mathbf{x}^{(1)}$ with *integer coordinates* are *lattice points* (marked by the index *L*). In this case the origin of the transformation is a lattice point. According to (1) every lattice point in lattice 1 has a partner in lattice 2.

Now, lattice 1 can be imaged on to the *same* lattice 2 by means of the *same* transformation **A**, but starting from *other* origins. The pairing of lattice points will be different. We define the *O-lattice* as the *lattice of all these possible origins*. It is determined as the solutions of the equation

$$\mathbf{b}^{(L)} = (\mathbf{I} - \mathbf{A}^{-1})\mathbf{x}^{(O)} \tag{2}$$

$\mathbf{I}$ = unit transformation (identity)
$\mathbf{x}^{(O)}$ = *O*-point
$\mathbf{b}^{(L)}$ = translation vector of lattice 1.

Instead of dealing with the translation vectors of lattice 1 (*i.e.* difference vectors between lattice points), we may imagine that all these translation vectors are taken out of lattice 1 and that they are translated so that they start at a common origin. In this way we reconstruct lattice 1 in structure and orientation and we call this lattice (of all translation vectors of lattice 1) the *b-lattice* and consider (2) as an *imaging relation* between the *O*- and *b*-lattice. Hence $\mathbf{b}^{(L)}$ means a lattice vector of the *b*-lattice.

If the determinant

$$|\mathbf{I} - \mathbf{A}^{-1}| \neq 0 \ , \tag{3}$$

the *O*-lattice is given by

$$\mathbf{x}^{(O)} = (\mathbf{I} - \mathbf{A}^{-1})^{-1}\mathbf{b}^{(L)} \ . \tag{4}$$

Since we refer to lattice 1 as the basic coordinate system, the $\mathbf{b}^{(L)}$ vectors have integer coordinates and the *unit cell* of the *O*-lattice, as image of the unit cell of the *b*-lattice, is given by the column vectors of the matrix $(\mathbf{I} - \mathbf{A}^{-1})^{-1}$. These column vectors may also be expressed in orthogonal coordinates for easier plotting and quantitative evaluation. There are two limiting cases in the *O*-lattice theory:

The first one occurs when the unit cell of the *O*-lattice is large compared with the one of the crystal lattice or the *b*-lattice respectively. In this case the boundary is formed by a dislocation network.

In the second limiting case the *O*-lattice unit cell is about the size of the unit cell of the *b*-lattice. Here the periodicity of the pattern of lattice points plays the crucial part (coincidence site lattice).

In our present study we are dealing only with the first case, *i.e.* with dislocation networks.

Characteristics of an optimal boundary

If there is a choice between different transformations ($\mathbf{A}, \mathbf{A}' \ldots$) for relating the two lattices, the transformation which relates the *nearest* neighbours is the one which produces the largest O-lattice and thus is the one with the smallest absolute value of the determinant $|\mathbf{I}-\mathbf{A}^{-1}|$.

On the other hand, if we have a transformation which already relates the nearest neighbours and vary it by changing the relative orientation of the two lattices, the orientation with the smallest determinant is *not* always the one corresponding to the optimal boundary.

The determinant $|\mathbf{I}-\mathbf{A}^{-1}|$ can become zero and change sign. The case of the zero determinant will be discussed below, but it can be said here that the O-lattice degenerates into a lattice consisting of parallel lines, *i.e.* the unit cell of the O-lattice becomes infinite.

The determinant $|\mathbf{I}-\mathbf{A}^{-1}|$ is a volume measure and is the volume ratio of the b- to the O-lattice unit cell. However, for a boundary we need a measure for a surface. The best measure would be the energy per unit boundary surface but it is unknown in most cases. As we are dealing with the *geometry* of grain boundaries we introduce here a *geometrical* parameter, which gives some indication of the boundary energy. If the boundary consists of a row of parallel dislocation lines (spacing d, Burgers vector $\mathbf{b}$), the surface energy E is

$$E=E_0\theta(K-\ln\theta) \text{ with } \theta=b/d \tag{5}$$

(Read, 1953). E_0 and K are material constants. $E(\theta)$ increases from the value $E=0$ for $\theta=0$ to a maximum for θ between 15° and 25° and decreases slightly afterwards. As soon as the dislocation density becomes too high, equation (5) looses its validity. This equation is also true for all kinds of low angle boundaries but with different constants E_0 and K.

As long as we restrict ourselves to locating a minimum of the surface energy without expecting numerical values of the energy, we can use a parameter with the only property of increasing monotonically with the surface energy, in the range of interest.

For a boundary consisting of two sets of parallel dislocations we choose as parameter

$$P=(b_1/d_1)^2+(b_2/d_2)^2 \tag{6}$$

P is expected to be a valid indication as long as the spacing of the O points is large compared with the crystal lattice spacings, which is the case in our problem.

Selecting as possible boundaries the three faces of the O-lattice unit cell, the corresponding geometrical parameters are:

$$P1=\frac{(|\mathbf{x}_2^{(O)}|\,.\,|\mathbf{b}_3^{(L)}|)^2+(|\mathbf{x}_3^{(O)}|\,.\,|\mathbf{b}_2^{(L)}|)^2}{|\mathbf{x}_2^{(O)}\times\mathbf{x}_3^{(O)}|^2}\,. \tag{7}$$

$P2$ and $P3$ are obtained by cyclic permutation of the indices. These parameters follow from the relation between the O-lattice, the b-lattice and the corresponding dislocation network as indicated elsewhere (Bollmann, 1962, 1964, 1967, p. 384). They are only justified if the boundary is a dislocation network which is the case in the present study (see *e.g.* Fig. 5).

The optimal boundary is obtained for the minimum value of the smallest of the parameters $P1$, $P2$ and $P3$.

Transformation A

The lattice constants $a, b, c, \alpha, \beta, \gamma$ of both structures are given. We start with an orthogonal coordinate system in Å (unit vectors $\mathbf{u}_k^{(\mathrm{orth})}$) in which the unit vectors of the crystal structures $\mathbf{u}_i^{(j)}$ are expressed.*

$$\mathbf{u}^{(j)}=(\tilde{\mathbf{S}}^{(j)})\mathbf{u}^{(\mathrm{orth})} \quad j=1,2\,. \tag{8}$$

We place the a axis into the x axis and the ac plane into the xz plane.† The coefficients can be determined by using the scalar products of the $u_i^{(j)}$. The matrix $\mathbf{S}$ which is the transposed matrix of $\tilde{\mathbf{S}}$‡ in (8), the column vectors of which are the unit vectors of the crystal coordinate system $(\mathbf{a},\mathbf{b},\mathbf{c})$ expressed in the orthogonal coordinates, becomes:

$$\left.\begin{array}{ll}
\mathbf{a} & S_{11}=a \\
 & S_{21}=0 \\
 & S_{31}=0 \\
\mathbf{b} & S_{12}=b\,.\cos\gamma \\
 & S_{22}=(b/\sin\beta)\,(\sin^2\beta-\cos^2\alpha-\cos^2\gamma \\
 & \qquad +\cos\alpha\cos\beta\cos\gamma)^{1/2} \\
 & S_{32}=(b/\sin\beta)\,(\cos\alpha-\cos\beta\,.\cos\gamma) \\
\mathbf{c} & S_{13}=c\,.\cos\beta \\
 & S_{23}=0 \\
 & S_{33}=c\,.\sin\beta
\end{array}\right\} \tag{9}$$

This is done for both structures. The second structure is then rotated independently around the x, y and z axes by a few degrees. Since the angles of rotation φ_i are small we use the approximation $\sin\varphi\simeq\varphi$, $\cos\varphi\simeq1$. Hence the right-hand rotation around the x axis is

$$\mathbf{R}_x=\begin{pmatrix}1 & 0 & 0\\ 0 & 1 & -\varphi_x\\ 0 & \varphi_x & 1\end{pmatrix} \tag{10}$$

and similarly for the rotations $\mathbf{R}_y$ and $\mathbf{R}_z$ around the y and the z axes (by cyclic permutation of the indices).

We start with an orthogonal lattice and transform it into the structure 1:

$$\mathbf{x}^{(1)}=\mathbf{S}^{(1)}\mathbf{x}^{(\mathrm{orth})}\,. \tag{11}$$

In accordance with this we produce structure 2:

$$\mathbf{x}^{(2)}=\mathbf{R}_z\mathbf{R}_y\mathbf{R}_x\mathbf{S}^{(2)}\mathbf{x}^{(\mathrm{orth})}\,. \tag{12}$$

---

* A good introduction to practical matrix calculation is given by Wayman (1964).

† It would have been preferable with regard to mineralogical conventions to place the c axis into the z axis.

‡ The transpose of a general matrix $\mathbf{M}$ is indicated by $\tilde{\mathbf{M}}$.

By eliminating $\mathbf{x}^{(\mathrm{orth})}$ we obtain

$$\mathbf{x}^{(2)}=\mathbf{R}_z\mathbf{R}_y\mathbf{R}_x\mathbf{S}^{(2)}(\mathbf{S}^{(1)})^{-1}\mathbf{x}^{(1)}:=\mathbf{A}^{(\mathrm{orth})}\mathbf{x}^{(1)}\,. \quad (13)$$

Here the whole equation is expressed in orthogonal coordinates.

In order to express it in the coordinate system of lattice 1 we have to transform $\mathbf{A}^{(\mathrm{orth})}$ by

$$\mathbf{A}^{(1)}=(\mathbf{S}^{(1)})^{-1}\mathbf{A}^{(\mathrm{orth})}\mathbf{S}^{(1)}\,, \quad (14)$$

i.e. $$\mathbf{x}^{(2)}=(\mathbf{S}^{(1)})^{-1}\mathbf{R}_z\mathbf{R}_y\mathbf{R}_x\mathbf{S}^{(2)}\mathbf{x}^{(1)}:=\mathbf{A}^{(1)}\mathbf{x}^{(1)}\,. \quad (15)$$

Now we form $(\mathbf{A}^{(1)})^{-1}$ which is:

$$(\mathbf{A}^{(1)})^{-1}=(\mathbf{S}^{(2)})^{-1}\mathbf{R}_x^{-1}\mathbf{R}_y^{-1}\mathbf{R}_z^{-1}\mathbf{S}^{(1)} \quad (16)$$

and

$$(\mathbf{I}-(\mathbf{A}^{(1)})^{-1})=(\mathbf{I}-(\mathbf{S}^{(2)})^{-1}\mathbf{R}_x^{-1}\mathbf{R}_y^{-1}\mathbf{R}_z^{-1}\mathbf{S}^{(1)})\,. \quad (17)$$

For the rotations, which are orthogonal transformations,

$$\mathbf{R}^{-1}=\tilde{\mathbf{R}}\,. \quad (18)$$

From here on the determinant $|\mathbf{I}-\mathbf{A}^{-1}|$ and the inverse matrix $(\mathbf{I}-\mathbf{A}^{-1})^{-1}$ are calculated. The column vectors of this matrix are the unit vectors of the *O*-lattice in the coordinate system of lattice 1 (where the *b*-unit vectors are of the type ⟨1,0,0⟩).

If we place the possible boundaries through the faces of the *O*-lattice unit cell we obtain the Miller indices of these planes (*i.e.* normal vectors in the reciprocal lattice of the crystal coordinate system) as vector product of the *O*-lattice unit vectors

$$n_1=[\mathbf{x}_2^{(O)}\times\mathbf{x}_3^{(O)}]\,,\ etc. \quad (19)$$

In order to calculate the geometrical parameters (7) we transform the *O*-lattice unit vectors, as well as those of the *b*-lattice back into the orthogonal coordinate system by

$$\mathbf{x}_i^{(O\text{-orth})}=\mathbf{S}^{(1)}\mathbf{x}_i^{(O)} \quad (20)$$

and similarly the *b*-vectors.

Organization of the calculation

The computer calculation is divided into two independent programs.

Program 1

Program 1 allows mapping of $|\mathbf{I}-\mathbf{A}^{-1}|$, $P1$, $P2$ and $P3$ (7) as a function of the angles of rotation φ_x, φ_y, φ_z. It consists essentially of the following steps.

(*a*) Input: a, b, c, α, β, γ of the two lattices.
(*b*) Calculation of $\mathbf{S}^{(1)}$ and $\mathbf{S}^{(2)}$ (9) and their determinants.
(*c*) $\det\mathbf{S}^{(2)}/\det\mathbf{S}^{(1)}$ = volume ratio of the two unit cells.
(*d*) Input: φ-start, $\Delta\varphi$ and the number of steps for the 3 angles.
(*e*) Calculation of $\mathbf{A}^{-1}$, $(\mathbf{I}-\mathbf{A}^{-1})$, $|\mathbf{I}-\mathbf{A}^{-1}|$ and $(\mathbf{I}-\mathbf{A}^{-1})^{-1}$ in coordinates of lattice 1.
(*f*) Column vectors of $(\mathbf{I}-\mathbf{A}^{-1})^{-1}$, *i.e.* the unit vectors of the *O*-lattice and the corresponding *b*-vectors are transformed to orthogonal coordinates (20).
(*g*) $P1$, $P2$ and $P3$ are calculated (7).

The program prints the following results:

$$\mathbf{S}^{(1)},\ \det\mathbf{S}^{(1)},\ \mathbf{S}^{(2)},\ \det\mathbf{S}^{(2)},\ \det\mathbf{S}^{(2)}/\det\mathbf{S}^{(1)}\,.$$

As a table are given

$$\varphi_x,\ \varphi_y,\ \varphi_z,\ \det(\mathbf{I}-\mathbf{A}^{-1}),\ P1,\ P2,\ P3\,.$$

Maps are plotted of the different parameters from these tables, and from these maps specific values of the rotation angles φ are determined, for which the actual *O*-lattice is calculated This calculation is done in program 2. Before discussing this latter program we have to investigate the situation which arises when the determinant $|\mathbf{I}-\mathbf{A}^{-1}|$ becomes zero.

Situation when $|\mathbf{I}-\mathbf{A}^{-1}|=0$

When the determinant $|\mathbf{I}-\mathbf{A}^{-1}|$ is zero with the matrix acquiring rank 2, equation (2), which is a set of inhomogeneous linear equations, has solutions only for *b*-lattice points within a plane through the origin of the *b*-space. This plane is given by a linear relation between the values of $b_1^{(L)}$, $b_2^{(L)}$ and $b_3^{(L)}$ which makes the system of equation (2) soluble. We call this plane the *b*-subspace.

The transformation $\mathbf{A}$ in this case has an invariant axis, *i.e.* an eigenvector with the eigenvalue 1. The *O*-lattice degenerates into a line lattice with lines parallel to that eigenvector. Every point on these lines is an *O*-point, *i.e.* a solution of equation (2). We call an *O*-line, as element of the *O*-lattice, an *O-element*. Hence, by calculating the eigenvalues of $\mathbf{A}$ and the eigenvector for an eigenvalue close enough to 1, the orientation of the *O*-line within the interpenetrating lattices is given.

Once the orientation of the *O*-lines is known, their position has to be determined. Here the situation becomes more delicate. As mentioned above every *b*-lattice point lying within the *b*-subspace has an *O*-element as image. If the *b*-subspace lies arbitrarily within the *b*-lattice, only a few *b*-lattice points or even none at all may lie within that subspace. In terms of a dislocation network this would mean a boundary consisting of very few dislocations, each with an immense Burgers vector. Nature does not behave like this. In order to describe the real situation we have to widen the frame of the allowed transformations $\mathbf{A}$ so as to include also *inhomogeneous* transformations, *i.e.* those containing a translation. In this case the lattice points of the *b*-lattice in the near surroundings of the *b*-subspace can be projected perpendicularly on to the *b*-subspace* and the images of these projected points

---

* In the earlier paper (Bollmann, 1967) it was stated that the projection has to be done along the *O*-line. It has been found meanwhile that this procedure can lead to physically unstable situations.

determine the position of the O-elements. The transformation then consists of a homogeneous part plus a translation by the amount and direction of the projection of the b-lattice point on to the b-subspace. Hence, for all the O-elements the homogeneous part is the same but the translation differs from one O-element to another.

Program 2

(*a*) Input: matrices $\mathbf{S}^{(1)}$ and $\mathbf{S}^{(2)}$ calculated in program 1.
(*b*) Calculation of the metric tensor $\mathbf{G}$ of lattice 1. $\mathbf{G}=\tilde{\mathbf{S}}^{(1)}\mathbf{S}^{(1)}$.
(*c*) Calculation of $\mathbf{G}^{-1}$.
(*d*) Calculation of basis vectors of the reciprocal lattice.

$$\mathbf{a}^* = \frac{\mathbf{b}\times\mathbf{c}}{\mathbf{a}\,.\,[\mathbf{b}\times\mathbf{c}]}\ ,\ etc.$$

(*e*) Input: φ_x, φ_y, φ_z.
(*f*) Calculation of $\mathbf{A}$, $(\mathbf{I}-\mathbf{A}^{-1})$ and $(\mathbf{I}-\mathbf{A}^{-1})^{-1}$.
(*g*) Calculation of eigenvalues λ of $\mathbf{A}$, *i.e.* $|\mathbf{A}-\lambda\mathbf{I}|=0$.

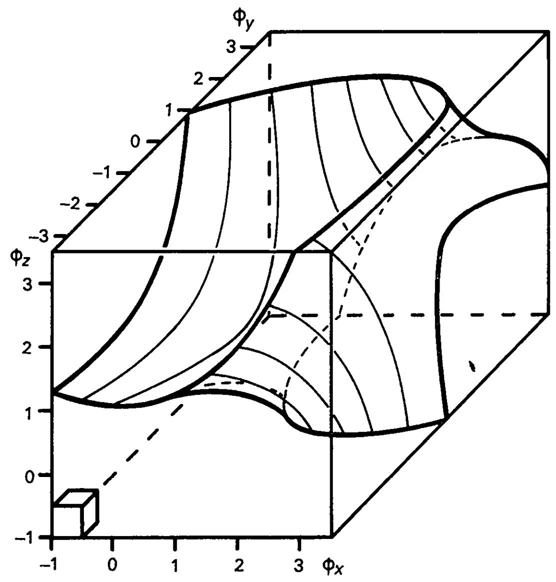

Fig. 2. Surface $|\mathbf{I}-\mathbf{A}^{-1}|=0$ as a function of the angles of rotation $\varphi_x, \varphi_y, \varphi_z$ (in degrees). Inside this 'hyperboloid' the determinant is positive, outside it is negative.

(*h*) Calculation of eigenvectors $\mathbf{x}^{(e)}$, $(\mathbf{A}-\lambda\mathbf{I})\mathbf{x}^{(e)}=0$, normalization to unit length and expression in lattice 1 and in orthogonal coordinates.
(*i*) If the eigenvalue is close enough to 1 the normal to the b-subspace is calculated, normalized to unit length and expressed in coordinates of lattice 1 as well as in orthogonal coordinates.

The normal on the b-subspace $\mathbf{b}^{(n)}$ can be calculated in the following way: let us consider (2) as a general relation between the x- and the b-space:

$$(\mathbf{I}-\mathbf{A}^{-1})\mathbf{x} := \mathbf{T}\mathbf{x} = b\,. \tag{21}$$

Every vector $\mathbf{x}$ has its image in the b-subspace. Hence we choose two unit vectors $\mathbf{x}[100]$ and $\mathbf{x}[010]$. Their images are $\mathbf{b}(T_{11}, T_{21}, T_{31})$ and $\mathbf{b}(T_{12}, T_{22}, T_{32})$. The vector product of these two vectors gives the coordinates of $\mathbf{b}^{(n)}$ in the reciprocal lattice. The absolute length of $\mathbf{b}^{(n)}$ can be determined by means of the inverse of the metric tensor

$$|\mathbf{b}^{(n)}|^2 = \tilde{\mathbf{b}}^{(n)}\mathbf{G}^{-1}\mathbf{b}^{(n)}\,. \tag{22}$$

After normalizing the vector it is transformed to the coordinate system of lattice 1 by

$$\mathbf{b}^{(n-1)} = \mathbf{G}^{-1}\mathbf{b}^{(n)}\,, \tag{23}$$

and to the orthogonal coordinate system by

$$\mathbf{b}^{(n\text{-orth})} = \mathbf{S}^{(1)}\mathbf{b}^{(n-1)}\,. \tag{24}$$

(*j*) Calculation of the angle α between the normalized eigenvector $\mathbf{x}^{(e)}$ and $\mathbf{b}^{(n-1)}$ by:

$$\cos\alpha = \tilde{\mathbf{x}}^{(e)}\mathbf{G}\mathbf{b}^{(n-1)}\,. \tag{25}$$

(*k*) The b-unit vectors [1,0,0] and [0,0,1] are projected on to the b-subspace along the direction of $\mathbf{b}^{(n-1)}$ in the coordinate system of lattice 1. We call these projected vectors $\mathbf{b}^{(Lp)}$. These unit vectors were chosen because it was found that the orientation of the b-subspace was nearest to the (010) plane.
(*l*) Now, the b-subspace with these projected unit vectors is rotated into the (ac) or (xz) plane respectively (so that $\mathbf{b}^{(n)}$ coincides with the y axis). $(\mathbf{I}-\mathbf{A}^{-1})$ is transformed correspondingly, then the y-components (second column and second line) are dropped so that $(\mathbf{I}-\mathbf{A}^{-1})$ becomes a two-dimensional transformation.

Table 1. *Lattice constants of the monoclinic and triclinic phases*

Structure	a (Å)	b (Å)	c (Å)	α	β	γ
Monoclinic 'Orthoclase' Or 92 Lattice 1	8·561(6)	12·996(2)	7·193(4)	90°	116°1′	90°
Triclinic Low albite Kodarma Lattice 2	8·135(3)	12·788(3)	7·154(2)	94°14′	116°31′	87°43′

(*m*) With this two-dimensional transformation the points where the *O*-lines cross the *xz* plane are obtained by:

$$\mathbf{x}^{(O)} = (\mathbf{I} - \mathbf{A}^{-1})^{-1}\mathbf{b}^{(Lp)} . \qquad (26)$$

(*n*) A further rotation brings the *O*-lines (*i.e.* $\mathbf{x}^{(e)}$) parallel to the *y* axis, so that their arrangement can be plotted.

Results

First we consider the adaptation of the monoclinic and the triclinic system and then that of two monoclinic systems.

Monoclinic–triclinic

The calculation is based on the lattice constants given in Table 1 for the two materials, taken from Cole, Sørum & Kennard (1949) (lattice 1) and Cole, Sørum & Taylor (1951) (lattice 2).

As the differences of the two lattices are too small for a drawing, we give here the matrices $\mathbf{S}^{(1)}$ and $\mathbf{S}^{(2)}$ the column vectors of which are the vectors **a**, **b** and **c** in the orthogonal coordinate system and as such can be plotted. The units are given in Å.

$$\mathbf{S}^{(1)} = \begin{array}{ccc} \mathbf{a}^{(1)} & \mathbf{b}^{(1)} & \mathbf{c}^{(1)} \\ \left(\begin{array}{ccc} 8{\cdot}562 & 0 & -3{\cdot}155 \\ 0 & 12{\cdot}996 & 0 \\ 0 & 0 & 6{\cdot}465 \end{array}\right) \end{array} \qquad (27)$$

and

$$\mathbf{S}^{(2)} = \begin{array}{ccc} \mathbf{a}^{(2)} & \mathbf{b}^{(2)} & \mathbf{c}^{(2)} \\ \left(\begin{array}{ccc} 8{\cdot}135 & 0{\cdot}510 & -3{\cdot}210 \\ 0 & 12{\cdot}751 & 0 \\ 0 & -0{\cdot}821 & 6{\cdot}393 \end{array}\right) \end{array} \qquad (28)$$

Fig. 2 shows the surface $|\mathbf{I} - \mathbf{A}^{-1}| = 0$ as a function of φ_x, φ_y and φ_z. Outside this 'hyperboloid' the determinant is negative, inside it is positive. A negative determinant means a change from the right-hand *b*-coordinate system to a left-hand *O*-coordinate system and, as already mentioned, a zero determinant indicates a degeneration of the *O*-lattice into a line lattice.

Fig. 3 shows two surfaces of constant value of the lowest of the geometrical parameters, which in this case is *P*1. The important feature is that two separate minima exist, *i.e.* two different relative orientations of the crystals with an optimal boundary. The deviations from the starting orientation [definition of matrices $\mathbf{S}^{(1)}$ and $\mathbf{S}^{(2)}$, equations 9, (27), (28)] are

	φ_x	φ_y	φ_z	*P*1
Optimum 1 φ'	2·125°	−0·529°	−0·464°	$26{\cdot}176 \times 10^{-4}$
Optimum 2 φ''	1·660°	2·757°	2·276°	$26{\cdot}925 \times 10^{-4}$
Difference $\varphi'' - \varphi' = \Delta$	−0·465°	3·286°	2·740°	3·5%
$\lvert\Delta\rvert$		4·3°		

The positions of vectors $\mathbf{a}^{(2)}$, $\mathbf{b}^{(2)}$ and $\mathbf{c}^{(2)}$ for the two optima are given as matrices:

$$\text{Optimum 1} \quad R'\mathbf{S}^{(2)} = \begin{array}{ccc} \mathbf{a}^{(2)\prime} & \mathbf{b}^{(2)\prime} & \mathbf{c}^{(2)\prime} \\ \left(\begin{array}{ccc} 8{\cdot}135 & 0{\cdot}044 & -3{\cdot}262 \\ 0{\cdot}320 & 12{\cdot}76 & -0{\cdot}060 \\ 0{\cdot}036 & -0{\cdot}935 & 6{\cdot}367 \end{array}\right) \end{array} \qquad (29)$$

and for

$$\text{Optimum 2} \quad R''\mathbf{S}^{(2)} = \begin{array}{ccc} \mathbf{a}^{(2)\prime\prime} & \mathbf{b}^{(2)\prime\prime} & \mathbf{c}^{(2)\prime\prime} \\ \left(\begin{array}{ccc} 8{\cdot}135 & 0{\cdot}106 & -2{\cdot}956 \\ 0{\cdot}236 & 12{\cdot}804 & -0{\cdot}491 \\ -0{\cdot}323 & -0{\cdot}229 & 6{\cdot}520 \end{array}\right) \end{array} , \qquad (30)$$

with R' and R'' representing the corresponding rotations by φ' and φ'' respectively from the starting position (28). In order to see the relative orientation of the

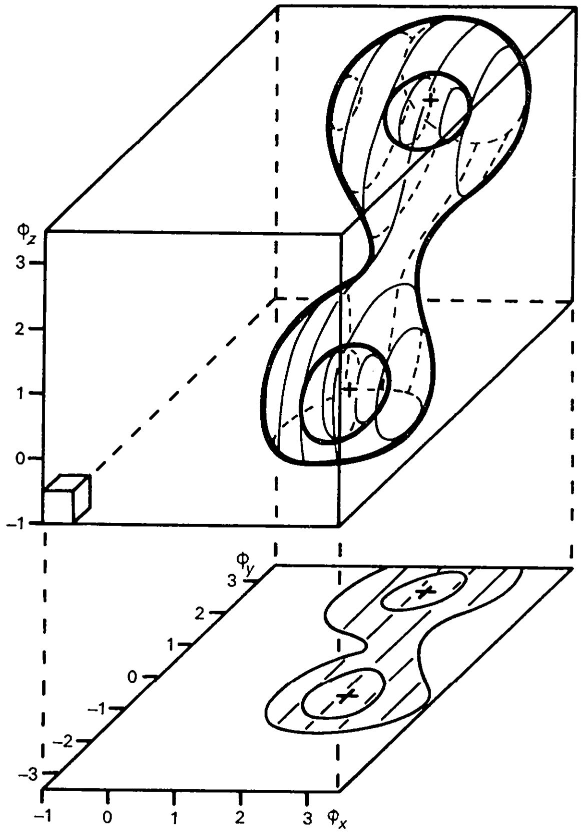

Fig. 3. Geometrical parameter *P*1 as a function of the angles of rotation. The outer connected surface corresponds to $P1 = 33 \times 10^{-4}$, the inner disconnected one to $P1 = 28 \times 10^{-4}$. Hence two separate minima of *P*1 exist.

two phases (29) or (30) can be plotted together with (27).

The values of $P1$ are nearly the same, which means that within the frame of the approximation used both minima have practically the same energy. Both minima lie very close to, but according to the calculation definitely not on, the surface of $|\mathbf{I}-\mathbf{A}^{-1}|=0$. The difference (optimum point to the nearest point on the surface) is:

Optimum 1 $(\;0{\cdot}003°,\; -0{\cdot}017°,\; -0{\cdot}010°)$
Optimum 2 $(-0{\cdot}025°,\; 0{\cdot}067°,\; 0{\cdot}049°)$.

Both optima have positive $|\mathbf{I}-\mathbf{A}^{-1}|$, *i.e.* they lie inside the surface shown in Fig. 2. The unit cells of the optimum *O*-lattices are very elongated owing to their closeness to the zero determinant surface. They are (in orthogonal coordinates):

Optimum 1 $\mathbf{x}_1^{(O)}=(-\;4697,\; -2659,\; 2371)$ Å
$\mathbf{x}_2^{(O)}=(\;16966,\; 9830,\; -9024)$ Å
$\mathbf{x}_3^{(O)}=(-10513,\; -6263,\; 5466)$ Å

Optimum 2 $\mathbf{x}_1^{(O)}=(-1290,\; 2837,\; 3598)$ Å
$\mathbf{x}_2^{(O)}=(-1412,\; 3304,\; -4506)$ Å
$\mathbf{x}_3^{(O)}=(\;896,\; -2192,\; 2643)$ Å

The plane indices of the optimum boundaries (*i.e.* the coordinates of the plane normals in the reciprocal lattice) are:

Optimum 1 $(3{\cdot}51\quad -4{\cdot}01\quad 1{\cdot}52)$
Optimum 2 $(1{\cdot}38\quad 0{\cdot}62\quad -0{\cdot}61)$

We see that in both cases these indices are completely different from the measured indices (Bøggild, 1924) which lie between $(60\bar{1})$ and $(80\bar{1})$.

Monoclinic–monoclinic

We further consider the case of the adaption of two monoclinic systems. As Laves (1952) has shown, a pseudo-monoclinic system can be produced out of a triclinic by averaging over periodic twinning. Two kinds of twinning are known which permit this transition:

1. *Twinning after the albite law* with rotation by 180° around a twin axis in the **b*** direction.
2. *Twinning after the pericline law* with the same rotation around an axis in the **b** direction.

In case 1, the *a* and *c* components of the **b** vector are set to 0, *i.e.*

$$S^{(2)}_{12}=S^{(2)}_{32}=0\,. \tag{31}$$

In case 2, the column vectors of the matrix $\mathbf{S}^{(2)}$ have to be rotated so that the *b*-vector coincides with the *y* axis (rotation **R**):

$$\mathbf{R}\,.\,\mathbf{S}^{(2)}=\mathbf{S}^{(2)\prime}\,. \tag{32}$$

Then the *b* components of the vectors **a** and **c** are set to 0.

$$S^{(2)\prime}_{21}=S^{(2)\prime}_{23}=0 \tag{33}$$

Fig. 4(*a*) shows a surface of constant value of the determinant $|\mathbf{I}-\mathbf{A}^{-1}|$ for albite twinning (the diagram is similar to that for pericline twinning) and Fig. 4(*b*) gives the corresponding diagram of the parameter $P1$. The interesting features are:

1. The determinant is always negative, *i.e.* never becomes zero.
2. The minimum of the absolute value of the determinant and the minimum of the lowest parameter, which here is $P1$, coincide for both kinds of twinning at the angular coordinate $\varphi(0°,\; 0{\cdot}93°(56'),\; 0°)$.
3. The values of $P1$ are:

   Albite twinning $P1=3{\cdot}94\times10^{-4}$
   Pericline twinning $P1=3{\cdot}27\times10^{-4}$

   The values of the minimum determinant are:

   Albite twinning $|\mathbf{I}-\mathbf{A}^{-1}|=-5{\cdot}7\times10^{-6}$
   Pericline twinning $|\mathbf{I}-\mathbf{A}^{-1}|=-7{\cdot}5\times10^{-6}$.

The determinant $|\mathbf{I}-\mathbf{A}^{-1}|$ is the inverse of the ratio: volume of *O*-lattice unit cell to volume of *b*-lattice unit cell. Therefore the *O*-lattice unit cell for albite twinning contains 175000 unit cells of the *b*-lattice (or lattice 1). For the pericline twinning this number is 133000.

The orientation of the phase boundary measured by Bøggild (1924) was reported to lie between the $(60\bar{1})$ and $(80\bar{1})$ orientations, *i.e.* both h_2 components are 0. These orientations correspond to an inclination of the plane normal with respect to the *x* axis in the (x,z) plane for

$(60\bar{1})$	14°28′
$(80\bar{1})$	17 49
Average	16 8·5
Deviation	±1 40

The calculated orientations are for the

Albite optimum	21°0·5′
Deviation from measured average	4 52
Pericline optimum	20 42
Deviation	4 33·5

Fig. 5 shows the details of the *O*-lattice, the corresponding *b*-lattice and the dislocation network of the optimal boundary for the pericline case. The albite case would be essentially the same but with somewhat different proportions. Fig. 6 shows a comparison of the optimum *O*-lattices for both kinds of twinning and the deviation of the calculated boundary orientation from the measured one.

Laves (1952) determined the directions in the (010) plane for which the angular deviation of the two joined phases is zero. The directions are close to [301] and [106]. Smith (1961) showed that these directions coincide with the maximum and minimum of the dilatational distortion. The direction of minimum dilatational distortion [106] lies in the plane of the phase boundary while [301] is perpendicular to it.

Mathematically expressed these directions must be eigenvectors of the optimum transformation $\mathbf{A}^{(\mathrm{opt})}$, *i.e.* solutions of the equations

$$\mathbf{A}^{(\mathrm{opt})}\mathbf{x} = \lambda_i \mathbf{x}$$

with the eigenvalues $\lambda_i (i = 1, 2, 3)$. The calculated eigenvalues for the albite average optimum are:

$$\lambda_1 = 0{\cdot}944, \quad \lambda_2 = 0{\cdot}980, \quad \lambda_3 = 0{\cdot}996\,.$$

The calculated orientations of the eigenvectors in the *ac* plane are: [2·56,0,1] (measured [3,0,1]) and [1,0,11·8] (measured [1,0,6]).

Fig. 7 shows a comparison between the measured and the calculated eigenvectors as well as between the corresponding boundary normals. We see that the calculated values differ from the measured ones but that the calculated eigenvector close to [106] coincides with the calculated boundary plane, while the calcu-

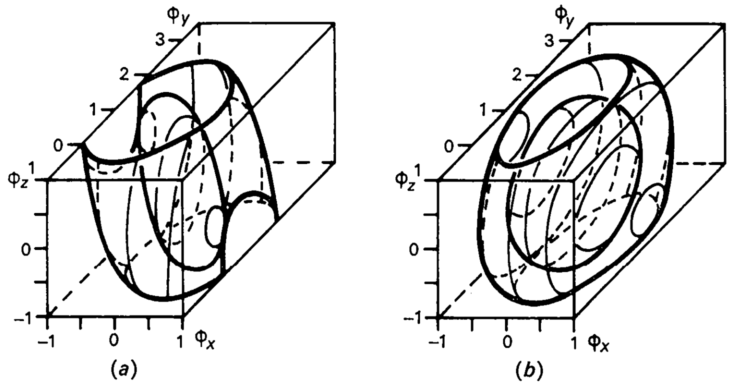

Fig. 4 (*a*) Surfaces of constant value of the determinant $|\mathbf{I}-\mathbf{A}^{-1}|$ for the albite average. Outer surface det $= -2\times10^{-5}$. Inner surface det $= -0{\cdot}85\times10^{-5}$. (*b*) Surfaces of constant value of the geometrical parameter *Pl* of the albite average. Outer surface $Pl = 91\times0^{-4}$. Inner surface $Pl = 6\times10^{-4}$. For the pericline average the corresponding pictures are of the same type.

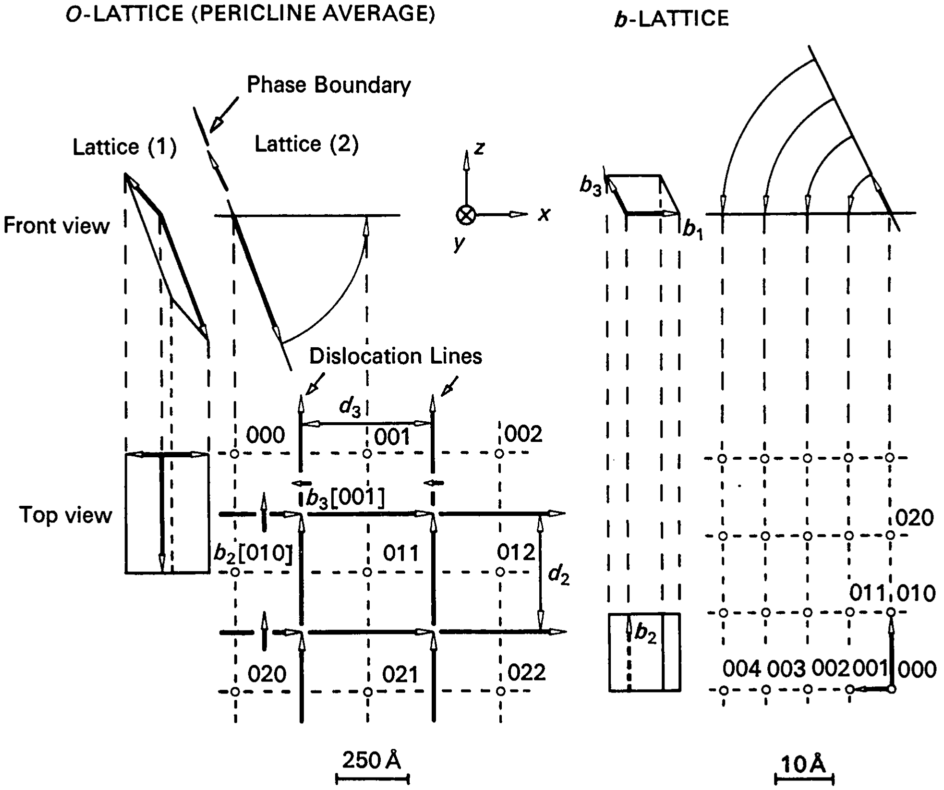

Fig. 5. *O*-lattice and dislocation network in the boundary for the pericline average. The case of the albite average is similar with somewhat different proportions.

lated eigenvector close to [301] stays nearly perpendicular to it. The third eigenvector lies in the *b* axis. We find that the eigenvector:

$\mathbf{x}(\lambda_2)$ coincides with $\mathbf{x}_2^{(O)}$ (*b* axis) and
$\mathbf{x}(\lambda_3)$ coincides with $\mathbf{x}_3^{(O)}$, but that
$\mathbf{x}(\lambda_1)$ differs completely from $\mathbf{x}_1^{(O)}$.

As we have seen, the optimal boundary is determined by $\mathbf{x}_2^{(O)}$ and $\mathbf{x}_3^{(O)}$. Since $(\lambda_i - 1) = \varepsilon_i$ is the dilatational distortion, the optimum boundary is determined here by the two eigenvectors (of the optimal transformation $\mathbf{A}^{(\mathrm{opt})}$) with the two smaller of the three $|\varepsilon_i|$ values. Hence, the boundary lies, as is to be expected, in the plane of minimum distortion.

Discussion and conclusions

On the basis of the *O*-lattice theory and the geometrical parameters $PI(I = 1,2,3)$ which, to a first approxi-

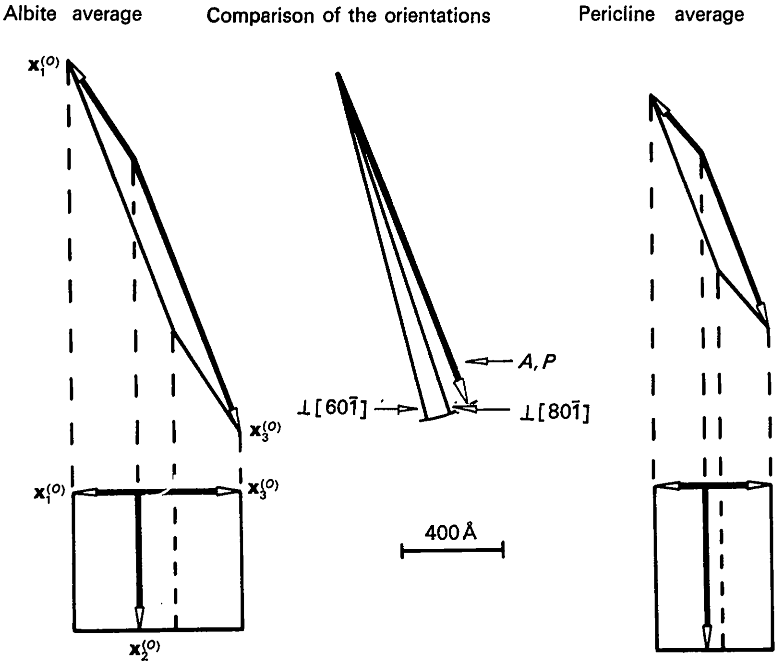

Fig. 6. Comparison of the optimum *O*-lattices for the albite and the pericline average. The calculated orientations *A*(albite), *P*(pericline) are compared with the measured ones.

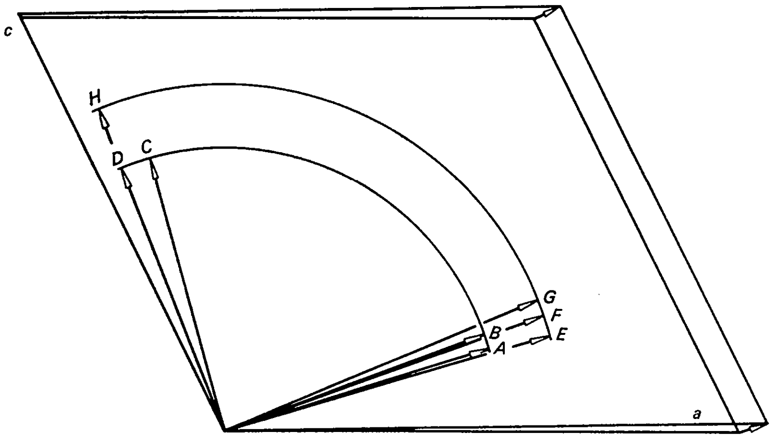

Fig. 7. Relative orientations of the unit cell for the albite optimum and comparison of the measured and calculated eigenvectors and boundary orientations. *A*, measured eigenvector [3,0,1]. *B*, calculated eigenvector [2·56,0,1]. *C*, measured eigenvector [1,0,6]. *D*, calculated eigenvector [1,0,11·8]. *E*, measured boundary normal (6,0,$\bar{1}$). *F*, measured boundary normal (8,0,$\bar{1}$). *G*, calculated boundary normal (12·6,0,$\bar{1}$). *H*, calculated direction of the boundary [1,0,11·8].

mation, are a measure of the surface energy of the boundary, the following results have been found for the two systems under consideration:

1. On adapting the monoclinic and the triclinic system, two optimal relative orientations of the two lattices exist. The corresponding *O*-lattices are nearly line lattices ($|\mathbf{I}-\mathbf{A}^{-1}|\simeq 0$). The orientations of the optimum boundaries are far off the measured values.
2. A triclinic structure can be transformed to an averaged monoclinic structure by periodic twinning. The twin law may be either the albite or the pericline law. For each case there exists only one optimal boundary and this lies in an orientation close to the measured one (deviations $\simeq 5°$). The parameter *P*1 is about 8 times lower than for the monoclinic–triclinic adaptation.

A comparison between the unit vectors of the *O*-lattice and the eigenvectors of the optimal transformation shows that the optimal boundary is determined by those two eigenvectors of the three which have the smaller dilatations. The fact that the orientation of the calculated boundary deviates from the measured one is due to the choice of the lattice constants of the two phases. A slight change in this choice could make the orientation fit exactly. Also a change of the parameters *PI* would influence the choice of the optimum.

On the basis of the geometrical parameters *PI* the twinned case is strongly favoured. On the other hand the formation of the twin boundaries increases the energy content of the material but (as the existence of the twinning as seen in Fig. 1 suggests) less than the decrease in phase boundary energy. The deviation of the triclinic lattice from the monoclinic is only about 4°, so that the twin boundary energy will be small.

The difference between the values for albite and for pericline twinning does not appear to be significant. Fig. 1 shows albite twinning while in our calculations a pericline twinning would be favoured and was found occasionally (see under *The Mineralogical Problem*). However, the orientation of the twin boundaries within the lamellae of the two-phase system plays a part and here the albite twinning is favoured as the twin boundary is perpendicular to the phase boundary, so that the twin boundary surface is minimized. This is not the case for pericline twinning.

An idea can be obtained about the sensitivity of the method from the fact that the difference between the albite and the pericline twinning induces a change of the *b* axes of 0·28% while the corresponding $\mathbf{x}_2^{(O)}$ values differ by 15%. The closer the two phases, the more sensitive is the calculation.

The theory applied here consists of two distinct parts. The first part is the determination of the *O*-lattice. For every orientation of the two crystals (*i.e.* for every point in the φ-space of Fig. 4) an *O*-lattice exists. The second part is the attribution of a 'measure' to the possible boundaries of the available *O*-lattices. In our case this is the attribution of the geometrical parameters *PI*. These parameters where kept as simple as possible. No splitting of dislocations into partials nor differences between edge- and screw-orientation were taken into account. A choice of another criterion might lead to other optimum points, *i.e.* to other *O*-lattices taken from the whole set which might then be judged the best.

It is to be stressed that all the results of this study were obtained *exclusively* from the six lattice constants of each of the two structures. No other numerical data were used, neither physical constants such as the elastic modulus nor atomic forces nor yet atomic coordinates. This means that the results *are independent* of such constants and that the same results would also be obtained if the given unit cells were filled with atoms in a completely different way.

The authors would like to express their thanks to Professors F. Laves and H. Nowotny for very inspiring discussions, Dr A. J. Perry for correcting the English, Miss S. Köppe for the execution of the drawings and the Battelle Institute for financing this work.

References

Alling, H. L. (1932). *Amer. Min.* **17**, 43.
Amelinckx, S. & Dekeyser, W. (1959). *Solid State Physics*, Vol. 8, p. 325. London and New York: Academic Press.
Bollmann, W. (1962). *Phil. Mag.* **7**, 1513.
Bollmann, W. (1964). *Discuss. Faraday Soc.* **38**, 26.
Bollmann, W. (1967). *Phil. Mag.* **16**, part I, 363; part **II**, 383.
Brandon, D. G. (1966). *Acta Metallurg.* **14**, 1479.
Brögger, W. C. (1890). *Z. Kristallogr.* **16**, 524.
Bøggild, O. B. (1924). *Kgl. Danske Videnskab. Selsk., Mat.-fys. Medd.* **6**, 1.
Chao, S. & Taylor, W. H. (1940). *Proc. Roy. Soc.* A **174**, 57.
Cole, W. F., Sørum, H. & Kennard, O. (1949). *Acta Cryst.* **2**, 280.
Cole, W. F., Sørum, H. & Taylor, W. H. (1951). *Acta Cryst.* **4**, 20.
Des Cloizeaux, A. (1862). *Manuel de Minéralogie*, Vol. I.
Des Cloizeaux, A. (1876). *Ann. Chim. Phys.* [5] **9**, 42.
Fleet, S. G. & Ribbe, P. H. (1963). *Phil. Mag.* **8**, 1179.
Frank, F. C. (1950). *Conference on the Plastic Deformation of Crystalline Solids (Mellon Institute)*, p. 150.
Frank, F. C. (1958). Cited by S. Ranganathan.
Hadding, A. (1921). *Lunds Univ. Årssk.* **2**, 17.
Ito, T. & Sodanaga, R. (1952). *Acta Cryst.* **5**, 441.
Jayaraman, A. (1959). *Proc. Indian Acad. Sci.* **50**, 349.
Kôzu, S. & Endô, Y. (1921). *Tohoku Imp. Univ. Sci. Repts.* [3] **1**, 1.
Laves, F. (1952). *J. Geol.* **60**, 549.
Laves, F. & Soldatos, K. (1963). *Z. Kristallogr.* **118**, 69.
Mäkinen, E. (1917). *Geol. Fören. Förh.* p. 121.
MacKenzie, W. S. & Smith, J. V. (1955). *Z. Kristallogr.* **40**, 707.
McConnel, J. D. C. (1965). *Phil. Mag.* **11**, 1289.
Michaelis de Sáenz, I. (1965). *Schweiz. Min. Petr. Mitt.* **45**, 103.
Nissen, H.-U. (1967). *Schweiz. Min. Petr. Mitt.* **47**, 1140.
Nissen, H.-U. & Bollmann, W. (1966). *Sixth Int. Congr. Electron Micr., Kyoto*, **1**, 591.

ORVILLE, P. M. (1967). *Amer. Min.* **52**, 55.
RAMAN, C. V., JAYARAMAN, A. & SRINIVASAN, T. K. (1950). *Proc. Indian Acad. Sci.* **32**, 123.
RANGANATHAN, S. (1966). *Acta Cryst.* **21**, 197.
READ, W. T. (1953). *Dislocations in Crystals*, p.155. New York: McGraw-Hill.
SAALFELD, H. (1952). *Neues Jb. Min., Abh.* **83**, 347 (esp. p.360–363).
SCHRÖDER, A. (1965). *Naturwiss.* **52**, 589.
SMITH, J. V. (1961). *Amer. Min.* **46**, 1489.
SMITH, J. V. & MACKENZIE, W. S. (1954). *Acta Cryst.* **7**, 380.
SMITH, J. V. & MACKENZIE, W. S. (1955). *Z. Kristallogr.* **40**, 733.
WAYMAN, C. M. (1964). *Introduction to the Crystallography of Martensitic Transformations.* New York: Macmillan.

Acta Cryst. (1968). A**24**, 557

Kinematical Diffraction from Solid Solutions with Short Range Order and Size Effect

BY J. M. COWLEY

School of Physics, University of Melbourne, Parkville, Victoria 3052, *Australia*

(*Received* 19 *December* 1967)

A new approach to the kinematical theory has been developed for the case of binary alloy solid solutions with short-range ordering of the atoms and displacements of the atoms from the average lattice sites due to departures of the effective atomic radii from the average for the alloy. Both the pseudo-temperature factor on the Bragg reflexions and the diffuse scattering intensity are shown to depend on summations over higher-order correlation parameters, defined in terms of the probabilities that groups of three, four or more sites should be occupied in specific ways. Expressions involving these parameters, and the usual short-range order parameters, α_i, are derived with terms of up to the second order in the displacement parameters for the Huang scattering around the fundamental Bragg reflexions, for the short-range order diffuse peaks, and for additional diffuse scattering depending on higher-order correlation parameters only. Special cases of practical significance are explored, and some estimates are made of the relative magnitudes of the terms not included in previous treatments of this problem.

Introduction

The usual treatment of the diffraction of X-rays, or of electrons or neutrons, by binary alloy solid solutions involves the kinematical or single-scattering approximation. The complications resulting from dynamical interactions of diffracted beams are treated elsewhere (Fisher, 1965; Cowley 1966; Cowley & Murray, 1968). The initial kinematical treatments (see *e.g.* Cowley, 1950) involved the assumption that the atoms were placed on the lattice points of a periodic space lattice. The fundamental reflexions that are given by both the fully ordered and completely disordered states were then found to be independent of the state of order. The intensities of the diffuse scattering due to short-range order (s.r.o.), or of the superlattice peaks given by alloys with partial long-range order, could be expressed in terms of Fourier series with the Warren s.r.o. parameters, α_i, (Cowley, 1950, 1965) as coefficients.

The modulation of the diffuse scattering arising from the static displacements of atoms which result from the differences in atomic sizes was first observed by Roberts (1954). Warren, Averbach & Roberts (1951) modified the diffraction theory by the inclusion of size-effect coefficients, β_i, which were dependent on the α_i and contributed an anti-symmetrical part to the s.r.o. diffuse peaks.

Later Borie (1957, 1959) gave a more complete account of the size effect, based on a treatment due to Huang (1947) of scattering from atomic displacements associated with point defects. Borie predicted four effects; the reduction of the intensity of fundamental reflexions by the equivalent of a temperature factor, the broadening of outer s.r.o. diffuse peaks, size-effect modulation and displacement of the s.r.o. diffuse peaks, and a Huang diffuse scattering around the fundamental peaks. Related results have been reported by Krivoglaz (1958), Krivoglaz & Tikhonova (1960), and by Smirnov & Tikhonova (1960).

While Borie showed that his predictions were in fair agreement with experimental observations, his treatment was based on some rather severe approximations. In dealing with the Huang scattering for example, he dealt only with the limiting case of a small degree of s.r.o. While this proved sufficient for a first comparison with experiment, and established the general form of the diffuse scattering, it is probably an insufficient basis for the deriving of the more accurate values for s.r.o. and size-effect coefficients which may be required, for example, for comparisons with the theoretical results of Clapp & Moss (1966, 1968).

In discussing the limitations of his treatment, Borie (1957) points out that a more complete account of the scattering would involve correlation coefficients of higher order than the usual s.r.o. parameters which